frontiers in Energy Research

METHODS
published: 03 January 2022
doi: 10.3389/fenrg.2021.813978

Experimental Study on Fracturing Fracture Deformation Mechanism of Shale Reservoir

*Zuping Xiang†, Yangyang Ding *†, Xiang Ao, Zhicong Zhong‡, Zhijun Li‡, Hui Xiao‡, Zhonghua Chen‡, Qianhua Xiao‡ and Xinjian Ma‡*

College of Petroleum and Natural Gas Engineering, Chongqing University of Science and Technology, Chongqing, China

OPEN ACCESS

Edited by:
Hui Zhao,
Yangtze University, China

Reviewed by:
Li Chengyong,
Chengdu University of Technology, China
Xiaoliang Zhao,
China University of Petroleum, China

***Correspondence:**
Yangyang Ding
2711800388@qq.com

†These authors have contributed equally to this work and share first authorship

‡These authors have contributed equally to this work and share last authorship

Specialty section:
This article was submitted to Advanced Clean Fuel Technologies, a section of the journal Frontiers in Energy Research

Received: *12 November 2021*
Accepted: *22 November 2021*
Published: *03 January 2022*

Citation:
Xiang Z, Ding Y, Ao X, Zhong Z, Li Z, Xiao H, Chen Z, Xiao Q and Ma X (2022) Experimental Study on Fracturing Fracture Deformation Mechanism of Shale Reservoir. Front. Energy Res. 9:813978. doi: 10.3389/fenrg.2021.813978

After large-scale sand fracturing of horizontal wells in shale gas reservoir, fracturing fractures will deform in the production process. However, fracture deformation will lead to the decrease in fracture conductivity and then cause the decrease of gas well productivity. Therefore, in order to evaluate the fracturing fracture deformation mechanism of shale reservoirs, the shale proppant-supported fracture deformation evaluation experiments were carried out under different proppant types, particle sizes, sanding concentrations, and closure pressure conditions, respectively, and the variation curves of fracture width was calculated by a stereomicroscope under different experimental conditions. Then based on the experimental results, the fracture sensitivity factors and fracture deformation mechanism were analyzed, and the deformation mechanisms of fracturing fractures affected by proppant embedding and crushing were studied emphatically. The analysis results of fracture sensitivity factors indicate that the larger the particle size and hardness of proppant, the lower the sand concentration, proppant embedded on the shale rock surface. Moreover, the deeper the proppant is embedded, the faster the fracture conductivity decreases. In addition, the greater the closure pressure, the more serious is the proppant embedment, and the faster the fracture width decreases. The analysis results of fracture deformation mechanism show that, on the on hand, under variable closure pressure, the proppant with larger hardness and larger particle size is used for fracturing, and the proppant embedded in the fracture surface is the main cause of fracture deformation. However, if only the sand concentration of the proppant in the fracture is changed, the fracture deformation is jointly dominated by the embedding and crushing of the proppant. On the other hand, under constant closure pressure, the main mechanism of fracture deformation is that the proppant is embedded into the fracture surface when the closure pressure is low, but if the closure pressure is high, the main mechanism of fracture deformation is the crushing and compaction of proppant.

Keywords: shale gas reservoir, fracture deformation, embedding and crushing, proppant, sand concentration, closure pressure

1 INTRODUCTION

As one of the unconventional oil and gas resources, shale gas reservoir has the characteristics of low porosity, low permeability, high stress, and so on (Tan et al., 2017; Lei et al., 2018; Zeng 2020; Ao et al., 2021), so the natural productivity of shale gas reservoir is very low. Horizontal well fracturing technology is an important and effective method to improve unconventional oil and gas productivity (Lei et al., 2020). However, in the production process of shale reservoir after sand fracturing, the fracturing fracture will produce a certain deformation and leads to the decrease in fracture conductivity (Sun et al., 2019), thereby affecting the productivity of shale gas wells. Consequently, it is necessary to study the deformation mechanism of shale fracturing support fracture in the production process.

There are many factors that cause shale reservoir fracturing fracture deformation, and many scholars at home and abroad (Boyer et al., 2014; Li et al., 2016; Liu et al., 2019; Ao et al., 2020) have carried out related research. In 2009, H. Abass et al. (2009) simulated the effect of small particle size proppant on fracture conductivity and optimized the number of fractures. Yang et al. (2021) derived the mathematical expressions of fracture conductivity and fracture width, and then studied the influence of proppant type, particle size, and sanding concentration on fracture conductivity. In 2017, Deng et al., 2017 studied the influence of proppant embedment in rocks with different particle sizes and same *in situ* stress on fracture permeability by numerical simulation. The numerical simulation method has strong nonlinearity and is relatively difficult to solve when considering many factors. However, the experimental method can intuitively observe the changes in fractures under different conditions and obtain more fracturing parameters, which is relatively easy. Therefore, most scholars still study the deformation mechanism of fractures by experimental methods. In 2012, Rivers M. et al. compared and analyzed the fracture width and fracture conductivity under different conditions by experimental methods. They found that the fracture width decreases with the increase in effective closure pressure and time, and the fracture conductivity and width will further degrade when cyclic loading is applied to the proppant. Guo and Zhang. (2011) believed that the degree of proppant embedding on the fracture surface increased with the increase of proppant particle size and closure pressure, while Xu et al. (2011) believed that the particle size of proppant had little effect on the conductivity of the fracture, which was obviously inconsistent. In 2018, based on the research by Guo and Zhang (2011), He et al. (2018) also used experimental methods to study the effects of closure pressure, proppant particle size and sand laying method on the fracture conductivity of tight sandstone, and the conclusions are consistent. In 2020, in order to study the stress sensitivity of artificial fractures and natural fractures under different sand concentration, Chen et al. (2020) carried out the stress sensitivity test of shale artificial fractures under variable confining pressure and variable flow pressure. The experimental results show that the proppant cannot only improve the fracture conductivity but also effectively reduce the stress sensitivity of artificial fractures. In the same year, Liu (2020) carried out a series of laboratory experiments to study the effects of proppant type, particle size, and sand concentration on fracture conductivity. The results indicate that the larger the proppant particle size and sand concentration, the greater is the fracture conductivity. From the above studies, it can be found that the conductivity of shale fracturing support fractures is affected by the type of proppant, the particle size of proppant, the closure pressure, and the sand concentration, which will further affect the deformation mechanism of fractures. Consequently, in the production process of shale gas wells, in order to make proppant-supported fractures effectively maintain its high conductivity, it is necessary to fully understand the deformation mechanism of fracturing support fractures under different conditions.

In this study, an experimental evaluation method of shale fracturing fracture deformation mechanism was designed, which is based on the three experiments including shale rock plate embedding test, proppant embedding depth calculation by stereomicroscope, and long-term fracture conductivity test. Then the shale rock samples of Longmaxi Formation in Sichuan Basin were taken as the study subjects and through the designed evaluation method of fracture deformation mechanism, a series of fracture conductivity curves and fracture width curves were measured under the conditions of proppant types, proppant particle size, sand concentration, and closure pressure, respectively. Finally, based on the experimental results, the fracture sensitivity factors and fracture deformation mechanism were discussed. The research results are expected to provide some theoretical guidance for the optimization of fracturing parameters in shale gas reservoirs.

2 EXPERIMENTAL EEQUIPMENT AND SCHEME

2.1 Experimental Samples and Equipment

2.1.1 Experimental Sample

Shale rocks from Longmaxi Formation in Sichuan Basin were used in the experiment, and then these shale rocks were processed into rock plates with specific shape and size by shale wire-electrode cutting equipment, as shown in **Figure 1**. Nitrogen was used as test fluid, and ceramsite and quartz sand were used as proppant materials.

2.1.2 Flow Conductivity Testing Facilities

The main device of the experimental equipment is the acid corrosion fracture conductivity evaluation instrument, which is produced in China. The model is DL-2000, the temperature test range is room temperature to 180°C, the closure pressure test range is 0.1–150 MPa, and the displacement pressure test range is 0.1–40 MPa. The diversion chamber is improved on the basis of the API (American Petroleum Institute) standard diversion chamber (**Figures 2**, **3**). The length and width of the diversion

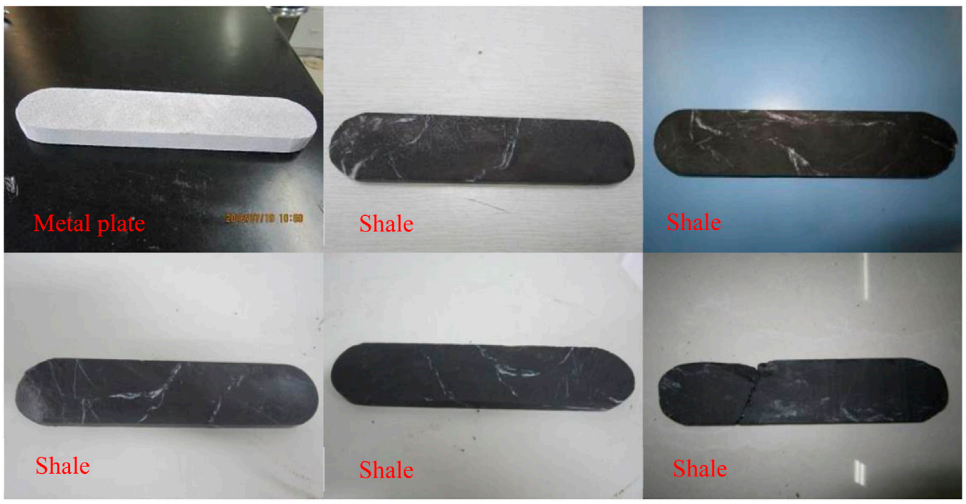

FIGURE 1 | Processed shale rock plates and metal plates.

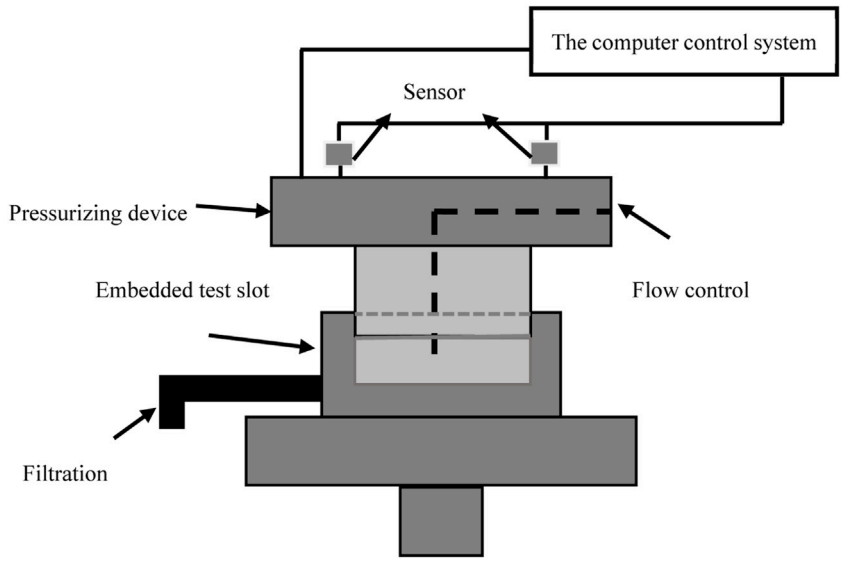

FIGURE 2 | Proppant embedding test device.

chamber are 100 and 40 mm (Wen et al., 2005; Zeng et al., 2020), respectively, and the depth adjustable range is 10–40 mm.

2.1.3 Embedding Depth Analysis Equipment

The pore diameter of proppant embedded in the core was measured by a stereomicroscope (Xianlin Technology, China, model EaScan-Q, accuracy: 25.0 μm) (**Figure 4**), and then the embedded depth of proppant was calculated.

2.2 Experimental Scheme Design

In this study, in order to realize the research purpose, a series of experimental schemes were designed as shown in **Table 1**, and the specific experimental steps are as follows:

1) Shale rock samples are processed into rock plates with length, width, and height of 100, 40, and 20 mm by shale wire-electrode cutting equipment, and then grind the two ports into smooth arcs. The experiment is carried out using the same shape and size of the steel plate as the contrast experiment sample.
2) First, the steel plate is put into the self-made diversion chamber, and the proppant is loaded into it. Then different closing pressures are applied to the test chamber with the proppant by hydraulic press. After the pressure is stable, nitrogen is used as the test fluid to test the permeability and conductivity of the proppant layer fractures.
3) Then the prepared shale rock plate is substituted for the steel plate, and the operation in step 2 is repeated to test the

FIGURE 3 | Shale rock plates in embedded test slot.

conductivity of the proppant-supported fracture under the same conditions.

4) After the embedding experiment, the rock plates for embedding test are taken out, and the diameter of the embedding section of the proppant is measured by stereomicroscope and scanning electron microscope equipment, and then the embedding depth of the proppant is calculated.
5) According to the experimental schemes, under different experimental conditions, steps 2 to 4 are repeated. When the closure pressure increases from 0 to 70 MPa (the pressure gradient is 5 MPa), the width, conductivity, and permeability of shale proppant-supported fracture after proppant embedding and crushing are tested and calculated, respectively (the test temperature is 24°C).

3 ANALYSIS ON INFLUENCING FACTORS OF FRACTURE CONDUCTIVITY AND FRACTURE WIDTH IN SHALE FRACTURING PROPPANT-SUPPORTED FRACTURE

3.1 Proppant Types

At present, ceramsite and quartz sand are widely used as fracturing proppant materials. Therefore, in this work, these two kinds of proppants were used to study the variation law of conductivity and fracture width of shale fracturing support fractures under different proppant types. Based on experimental schemes 1 and 2, the closing pressure is gradually increased in the range of 0–70 MPa and the gradient is 5 MPa, and then test the conductivity of shale rock and calculate the proppant embedding depth. The conductivity test results are shown in **Figure 5**, and the embedding depth calculation results are shown in **Figures 6** and **7**.

Figure 5 shows that the conductivity and permeability of the supporting fractures under the two types of proppants decrease

FIGURE 4 | EaScan-Q stereomicroscope.

with the increase in the closure pressure, but they do not change when they are reduced to a certain extent, and the permeability and conductivity of the fractures supported by quartz sand are always lower than those of the ceramsite.

Under different closure pressures, different types of proppants were embedded into the shale rock plates, and the shale rock plates were removed. The microscopic surface morphology of the rock after proppant embedding was observed under stereomicroscope (**Figure 6**), and then the embedding depth of the proppant was calculated (**Figure 7**). It can be seen in **Figure 6** that the number of ceramisite proppant embedded on the fracture surface was significantly more than that of quartz sand proppant. Moreover, as can be seen in **Figure 7**, with the increase in closure pressure, the embedding depth of the two types of proppants increases continuously, and the embedded depth of ceramsite in fractures is significantly higher than that of quartz sand. At the same time, the difference in embedded depth increases with the increase of closure pressure.

When the closure pressure is less than 50 MPa, with the increase in the closure pressure, the ceramic proppant with higher hardness is more easily embedded in the fracture with the increase in the closure pressure, resulting in fracture deformation. The quartz sand proppant with low hardness is not easy to be embedded with the increase in closure pressure in fracturing fractures, but it is more likely to be broken and compacted. However, the decrease rate of fracture conductivity caused by proppant crushing is higher than that caused by embedding. Therefore, the fracture conductivity and permeability of quartz sand support decrease faster with the increase in closure pressure. In addition, when the closure pressure is higher than 50 MPa, the effect of proppant

TABLE 1 | Parameter design of experimental schemes.

Numbers	Proppant types	Particle size of proppant (mesh)	Sanding concentration (kg/m^2)	Closure pressure (MPa)
1	Ceramsite	40/70	10	0–70
2	Quartz sand	40/70	10	0–70
3	Ceramsite	20/40	10	0–70
4	Ceramsite	40/70	10	0–70
5	Ceramsite	40/70	5	0–70
6	Ceramsite	40/70	7.5	0–70
7	Ceramsite	40/70	10	0–70
8	Ceramsite	40/70	15	0–70
9	Ceramsite	20/40	10	10
10	Ceramsite	20/40	10	20
11	Ceramsite	20/40	10	35
12	Ceramsite	20/40	10	50
13	Ceramsite	20/40	10	70

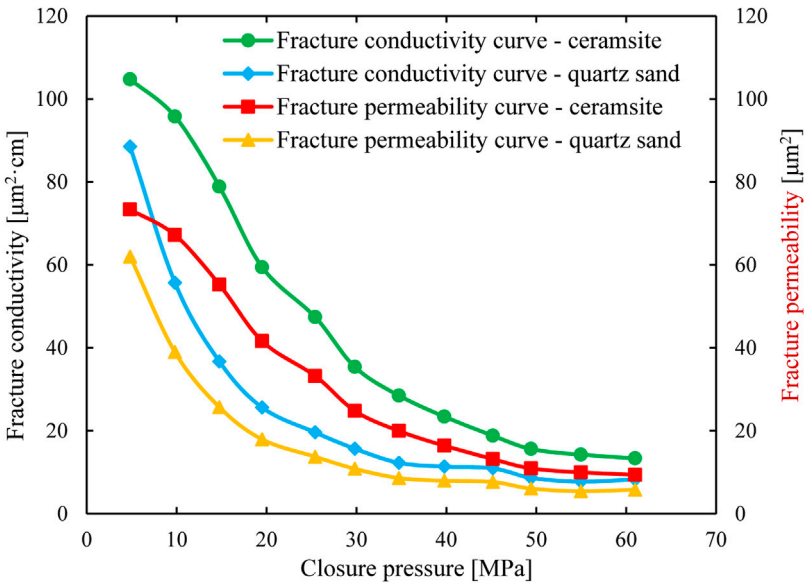

FIGURE 5 | Variation curves of fracture conductivity under different proppant types.

embedding, crushing, and compacting on the fracture width is small. Therefore, as the closure pressure continues to increase, the fracture conductivity under the two types of proppants almost no longer changes.

3.2 Particle size of proppant

Provided that the particle size of the proppant is different, the effect and the main position of the proppant in the fracturing process are different too. The proppant with large particle size is mainly used to support the main fractures and branch fractures, while the proppant with small particle size is mainly used to grind the pores, support micro fractures, and reduce the loss of fracturing fluid (Guo et al., 2008). However, the conductivity of fractures supported by proppants with different particle sizes is different, and the influence on fracture deformation is also different with the production. Consequently, based on the experimental schemes 3 and 4, in the closed pressure range of 5–70 MPa with 5 MPa as the gradient, the closed pressure test shale rock plate conductivity is gradually increased, and the proppant embedding depth is calculated. The conductivity test results are shown in **Figure 8**, and the embedded depth calculation results are shown in **Table 2**.

In **Figure 8**, it can be seen that with the increase in closure pressure, the conductivity and permeability of the fracture supported by these two kinds of particle size proppants decrease continuously, and the permeability and conductivity of 20/40 mesh ceramics are always higher than those of 40/70 mesh ceramics, but the conductivity of the fractures supported by larger particle size proppant decreases faster. However, when the closure pressure increases to a certain extent, the fracture

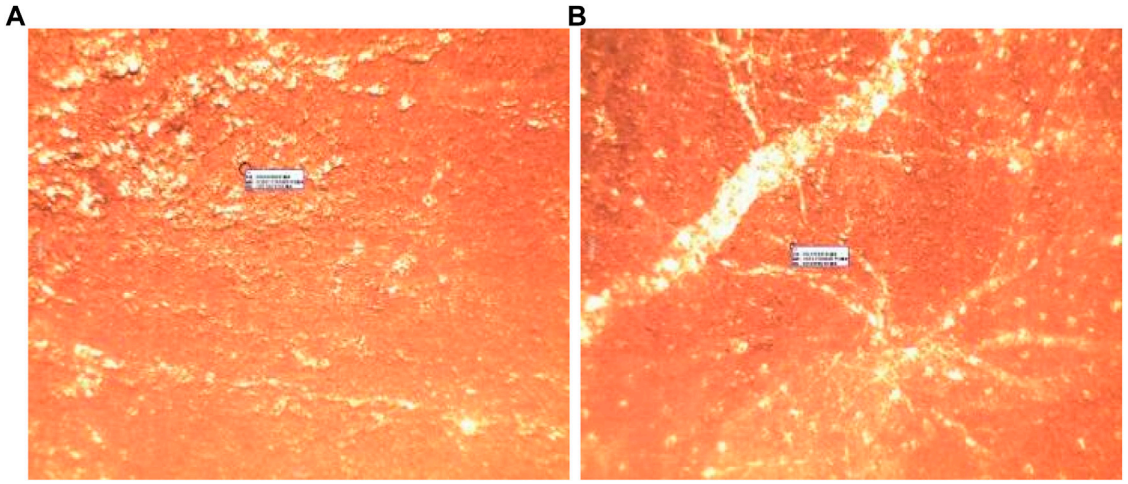

FIGURE 6 | Surface morphology of shale rock plates embedded with different types of proppant. **(A)** 20/40 mesh ceramsite proppant, **(B)** 20/40 mesh quartz sand proppant.

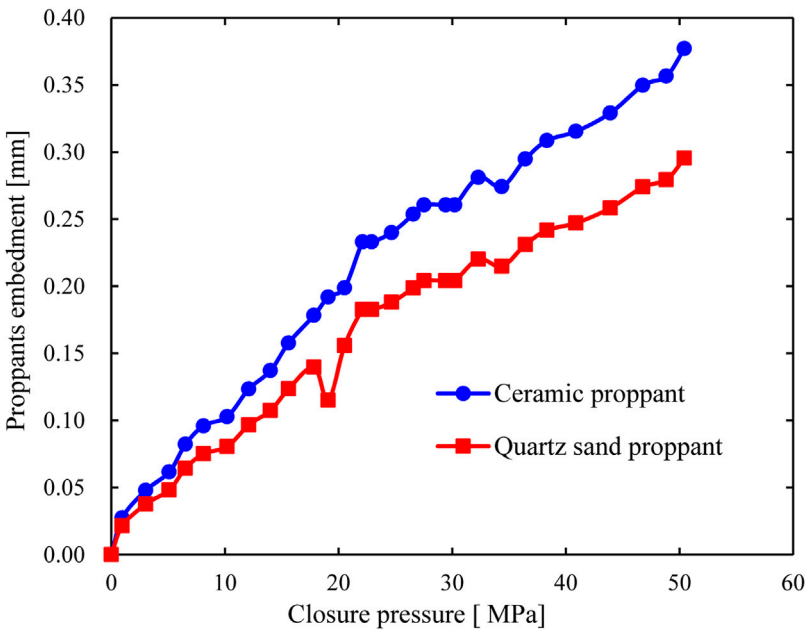

FIGURE 7 | Variation curves of proppant embedding depth under different proppant types.

conductivity does not change, and the fracture conductivity under the two particle size proppants is almost the same. The reason is that, when the closure pressure is lower than 55 MPa, with the increase in the closure pressure, the proppant layer is gradually compacted and embedded into the rock surface. Under the same conditions, the proppant with larger particle size is more likely to be embedded than the proppant with smaller particle size, so the fracture conductivity and permeability decrease faster, but with the increase in the deformation degree of the proppant, the advantages of the larger particle size proppant gradually disappear. When the pressure is higher than 55 MPa, the advantage of the larger particle size proppant almost completely disappears, so the conductivity of fracture supported by ceramsite proppant with particle size of 20/40 mesh and 40/70 mesh is almost the same and unchanged.

It can be seen from **Table 2** that the embedding depth of 20/40 mesh ceramics is slightly higher than that of 40/70 mesh ceramics, but the permeability and conductivity of the support fracture are higher than those of 40/70 mesh ceramics. Thus, the larger the particle size of the same type of proppant, the more serious the

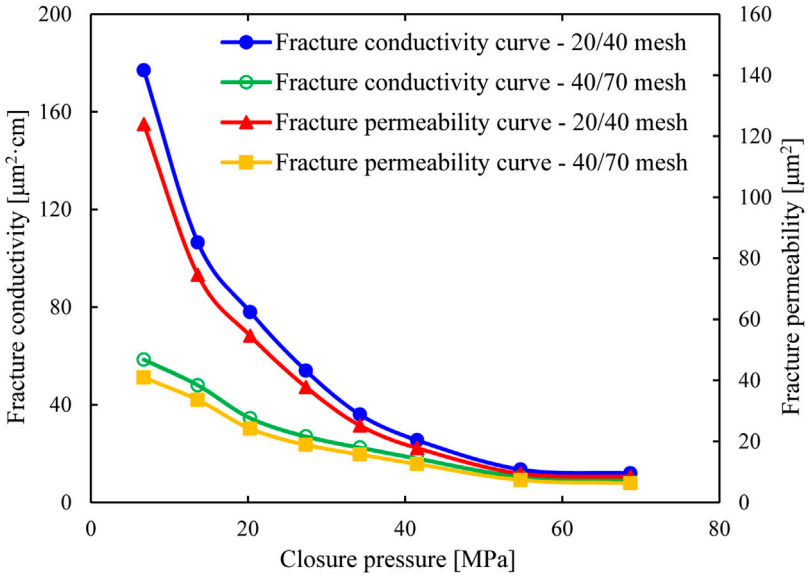

FIGURE 8 | Variation curves of fracture conductivity under different proppant particle sizes.

TABLE 2 | Embedding results of ceramsite proppants with different particle sizes at 55 MPa.

Schemes	Closure pressure (MPa)	Proppant types	Particle size of proppant (mesh)	Sanding concentration (kg/m^2)	Proppants embedment (μm)	Fracture permeability (μm^2)	Fracture conductivity (μm^2·cm)
3	55	Ceramsite	20/40	10	289	88	127
4	55	Ceramsite	40/70	10	207	75	107

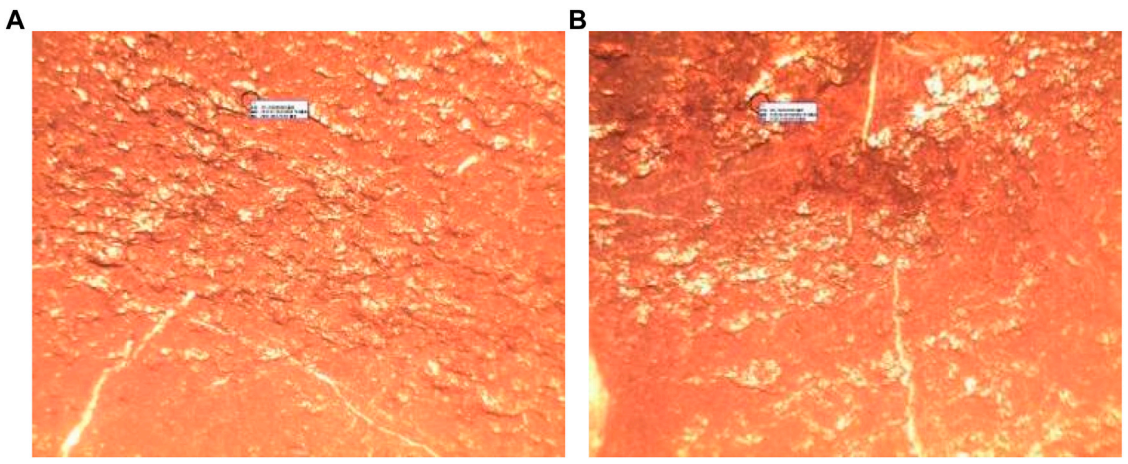

FIGURE 9 | Surface morphology of shale rock plates embedded with proppant under different sanding concentrations. **(A)** The sanding concentration is 5 kg/m^2. **(B)** The sanding concentration is 10 kg/m^2.

embedding is; this is consistent with the conclusions of Xu et al. (2019) and Wang et al. (2020). Under the same sand concentration, the larger the particle size of the same proppant is, the smaller the number of proppant particles in the unit area of fracturing fractures is, and the greater the closure pressure of each proppant is, the easier it is to embed into the fracture surface.

TABLE 3 | Embedding results under different paved-sand content.

Schemes	Closure pressure (MPa)	Proppant types	Particle size of proppant (mesh)	Sanding concentration (kg/m^2)	Proppants embedment (μm)	Fracture permeability (μm^2)	Fracture conductivity (μm^2·cm)
5	70	Ceramsite	20/40	5	283	60	85
7	70	Ceramsite	20/40	10	218	75	107

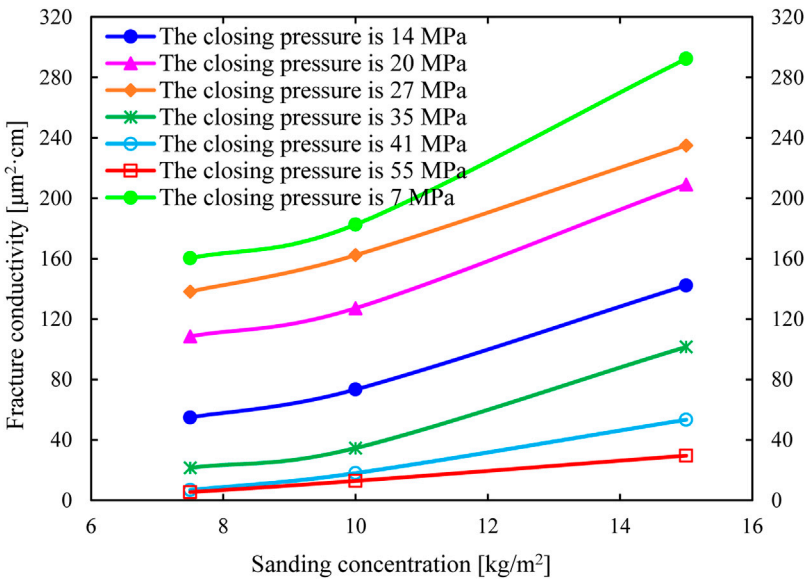

FIGURE 10 | Variation curves of fracture conductivity under different sanding concentration.

TABLE 4 | Embedding results under different closure pressures.

Schemes	Closure pressure (MPa)	Proppant types	Particle size of proppant (mesh)	Sanding concentration (kg/m^2)	Proppant embedment (μm)	Fracture permeability (μm^2)	Fracture conductivity (μm^2·cm)
9	10	Ceramsite	20/40	10	103	357	510
10	20	Ceramsite	20/40	10	199	270	386
11	35	Ceramsite	20/40	10	274	77.6	120
12	55	Ceramsite	20/40	10	380	59.5	85
13	70	Ceramsite	20/40	10	401	23.9	34

However, fractures with larger particle size proppants have wider initial width, resulting in greater conductivity and permeability.

3.3 Sand Concentration

Based on the experimental schemes 5, 6, 7, and 8, in the closed pressure range of 5–70, 5 MPa was used as the gradient to gradually increase the closed pressure to test the conductivity of shale rock plate and calculate the proppant embedding depth. The embedded depth calculation results are shown in **Figure 9** and **Table 3**, and the conductivity test results are shown in **Figure 10**.

Figure 9 and **Table 3** show that the embedded depth of proppant at sand concentration of 5 kg/m^2 is slightly higher than that at sand concentration of 10 kg/m^2, but the permeability and conductivity at sand concentration of 10 kg/m^2 are higher than those at sand concentration of 5 kg/m^2.

Figure 10 shows that with the increase in closure pressure, the conductivity and permeability of fracturing fractures decrease under different sand concentrations, and the diversion capacity of fractures under higher sanding concentration is always higher than those under low sand

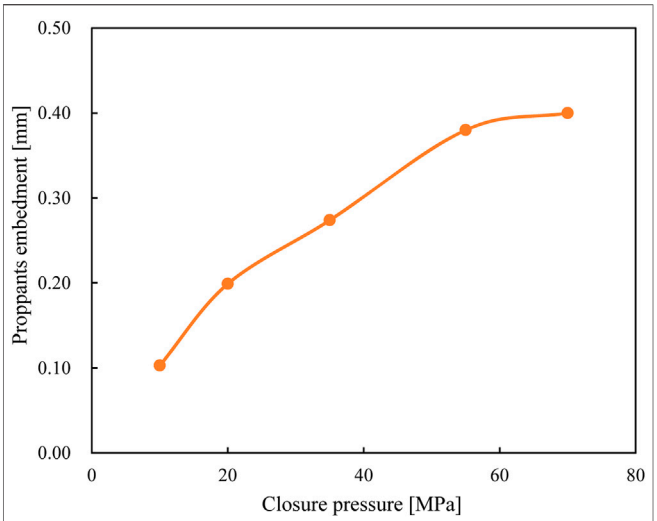

FIGURE 11 | Variation curve of embedding depth of ceramsite proppant under different closure pressures.

concentration. The analysis shows that the larger the sand concentration, the more the proppant layers in the fracture, the wider the initial fracture width, and the greater the conductivity of the fracture. Nevertheless, when the closure pressure is higher than 41.6 MPa, the proppant is crushed, the debris plugs the pores, and then increasing the sand concentration has little significance to improve the conductivity of the proppant-supported fracture. The higher the sand concentration is, the higher the requirements for the fracturing equipment are, and the greater the construction cost is. Therefore, it is necessary to optimize the sanding concentration according to the actual construction requirements and economic benefits.

3.4 Closure Pressure

Based on the experimental schemes 9 to 13, the long-term conductivity and permeability of shale rock plate proppant-supported fractures (48 h) were tested when the closure pressures were 10, 20, 35, 55, and 70 MPa, respectively. The test results are shown in **Table 4**, **Figure 11**, and **Figure 12**.

Table 4 and **Figure 11** show that the higher the closure pressure, the deeper is the proppant embedding, and the proppant embedding under high closure pressure is more serious; this is consistent with the conclusions of Zhao et al. (2017) and Chen et al. (2018). The embedding depth under 70 MPa is four times that under 10 MPa, and the fracture permeability and conductivity are reduced by 14 times. However, when the closure pressure is higher than a certain degree, the proppant will no longer be embedded.

We can see from **Figure 11** that with the increase in closure pressure, the fracture conductivity gradually decreases. When the test time is 24 h, under the low closure pressure, the conductivity decreases rapidly with the increase in time. When the closure pressure is higher than 55 MPa, the conductivity decreases slowly with the increase in time (**Figure 12**). In addition, When the test time was 48 h, when the closure pressure increased from 35 to 70 MPa, the diversion capacity decreased from 120 to 34 μm^2 cm, which decreased by 71.7%. It can be seen that when the closure pressure increases by 1 MPa, the conductivity decreases by an average of 0.97 μm^2 cm.

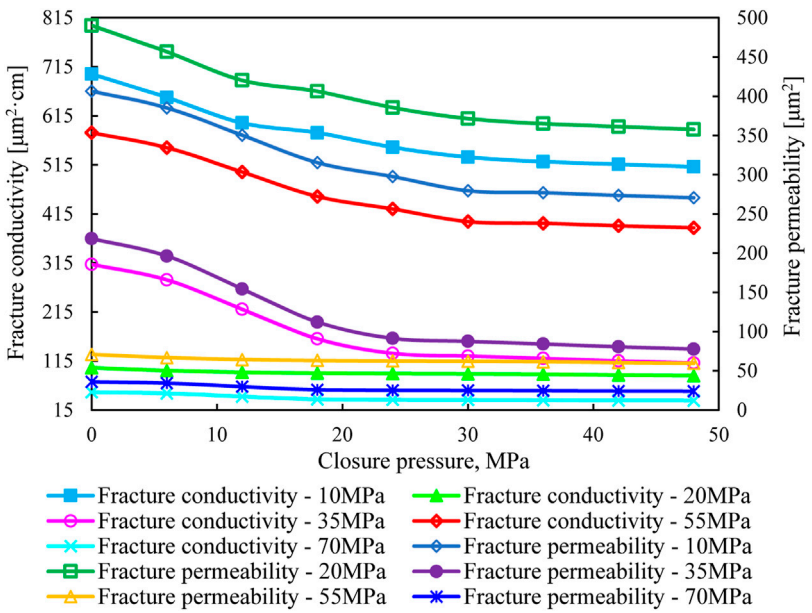

FIGURE 12 | Variation curves of fracture conductivity under different closure pressures.

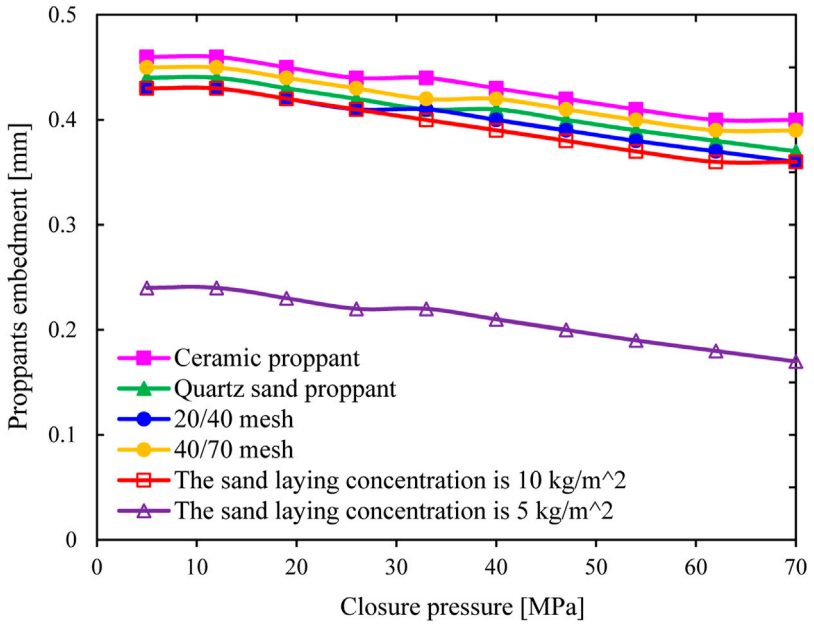

FIGURE 13 | Variation curves of fracture width with closure pressure under different conditions.

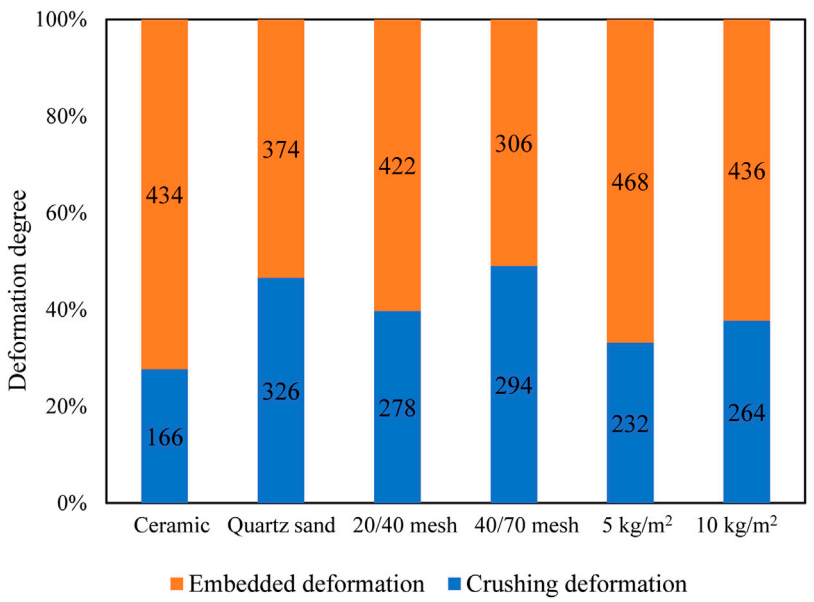

FIGURE 14 | Accumulation diagram of percentage contribution of embedding and crushing to fracture deformation under different conditions.

4 ANALYSIS OF SHALE FRACTURING FRACTURE DEFORMATION MECHANISM

4.1 Fracture Deformation Mechanism Under Variable Closure Pressure

Under different closure pressures, the degree of embedding and crushing of proppant in fractures is different, and the degree of fracture deformation is different too. Moreover, under different sand concentrations, proppant particle size, and hardness conditions, the degree of fracture deformation caused by proppant embedding and crushing is also different. Based on the experimental test results under different closure pressures, the results are shown in **Figures 13** and **14**. It can be seen from **Figure 13** that with the increase in closure pressure, the fracture width gradually decreases under different conditions. When the closure pressure reaches a certain degree, the fracture width

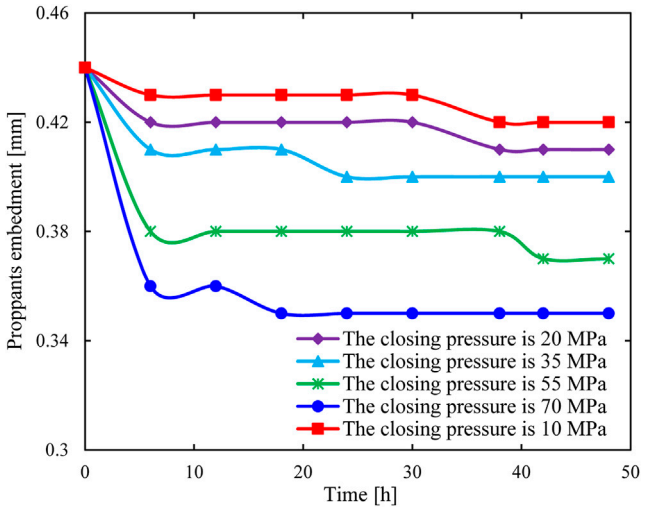

FIGURE 15 | Variation curves of fracture width with time under different closure pressure.

gradually tends to be flat. The influence of sand concentration on fracture width is the most obvious, and the fracture width increases with the increase of sand concentration.

It is assumed that the sum of the deformation variables of the caused by the embedding depth and crushing of the proppant under different conditions is 100%, the change values of fracture conductivity caused by proppant embedment and proppant breakage in the actual test are used to represent their respective proportions in the total fracture deformation, as shown in **Figure 14**. It can be seen in **Figure 13** that under the same closed pressure, the degree of fracture deformation caused by the embedding and crushing of ceramsite and quartz sand is compared. It is found that the embedding degree of ceramsite proppant with higher hardness in rock fractures is significantly higher than that of quartz sand with lower hardness, but the crushing degree of quartz sand in the same rock fractures is significantly higher than that of ceramsite. In addition, larger particle size proppant is more likely to be embedded than smaller particle size proppant. Moreover, when the large particle size proppant is crushed, it has a greater impact on the fracture width. Therefore, the embedding of proppant with high hardness and large particle size is the main reason for shale rock proppant-supported fracture deformation. Furthermore, under different sand concentration, the change of fracture width caused by proppant embedding and crushing is small, so the fracture deformation is caused by proppant embedding and crushing.

4.2 Fracture Deformation Mechanism Under Constant Closure Pressure

Based on the experimental test results, the variation law of fracture conductivity and the deformation mechanism of fracturing proppant-supported fracture under constant closure pressure are analyzed, and the results are shown in **Figures 15** and **16**.

Figure 15 shows that under the same closed pressure condition, with the experiment going on, the fracture width decreases rapidly at first and then slowly. When the test time exceeds 6 h, the fracture width changes slowly, and the greater the closure pressure is, the greater is the decrease of fracture width in the early experiment. **Figure 15** also indicates that when the test time exceeds 6 h, with the increase in test time, the fracture width

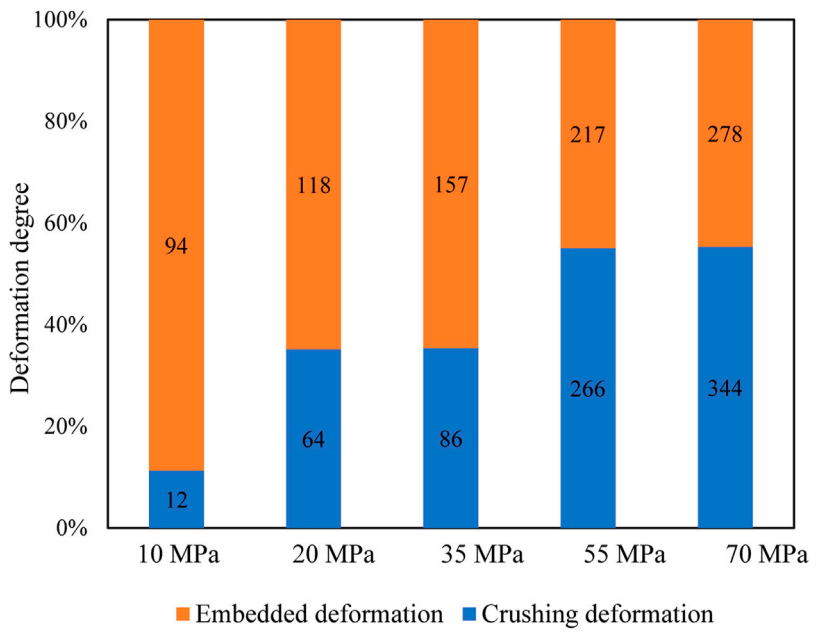

FIGURE 16 | Accumulation diagram of percentage contribution of embedding and crushing to fracture deformation under different closure pressures.

will further reduce and then tends to be stable. The reason is that the proppant is crushed due to the long-term closing pressure, resulting in the decrease in its supporting capacity, thereby reducing the fracture width and aggravating the degree of fracture deformation. **Figure 16** indicates that under low closure pressure, the fracture deformation caused by proppant embedding is much larger than that caused by crushing. However, with the increase in closure pressure, the proportion of proppant crushing deformation increases gradually, and the influence of crushing on fracture deformation is also increasing, which is gradually higher than that of embedding. **Figure 16** also shows that when the closure pressure is greater than 55 MPa, the influence of proppant embedding on fracture deformation is greatly reduced, but the proppant is seriously crushed. Therefore, the influence of crushing on fracture deformation increases rapidly and gradually plays a major role in fracture deformation. In summary, the fracture deformation of shale fracturing is mainly affected by proppant embedding under low closure pressure, and when the closure pressure is high, the fracture of proppant gradually becomes the main cause of fracture deformation.

CONCLUSION

In this work, by using the shale samples from the Longmaxi formation in the Sichuan Basin, and utilizing the designed experimental evaluation method of fracture deformation mechanism, the curves of fracture conductivity and fracture width of shale fracturing under different proppant types, proppant particle sizes, sand concentration, and closure pressure were measured. After that, based on the experimental results, the fracture sensitivity factors and deformation mechanism were studied. The main conclusions are as follows:

1) An experimental evaluation method for fracture deformation mechanism of shale fracturing is designed based on shale rock plate embedding test and stereomicroscope calculation of embedding depth, and combined with long-term fracture conductivity test, and the effective evaluation of deformation mechanism of shale fracturing proppant-supported fracture was realized.
2) The larger the proppant particle size, the greater the hardness, and the lower the sand concentration, the greater the embedded depth, which makes the fracture conductivity decrease faster. Moreover, the greater the closure pressure is, the deeper is the proppant embedding depth. However, when the closure pressure increases to a certain extent, the proppant embedding depth does not change.
3) Under variable closure pressure, the fracture deformation is mainly affected by proppant embedding when using proppant with larger hardness and larger particle size. In addition, under different sand concentrations, the deformation of fractures is affected by the embedding and crushing of proppant.
4) Under constant closing pressure, when the closing pressure is low, the fracture deformation of shale fracturing is mainly affected by proppant embedding. Nevertheless, when the closure pressure is high, the proppant crushed seriously, and the fracture deformation is mainly affected by the proppant crushing and compaction.

DATA AVAILABILITY STATEMENT

The raw data supporting the conclusion of this article will be made available by the author, without undue reservation.

AUTHOR CONTRIBUTIONS

YD conceptualized the study. YD and ZX handled the data curation and the preparation and writing of the original draft. HX, QX, and XM performed the experiments, YD, XA, and ZL polished the language of the article. YD, ZZ, and ZC conducted the literature research. All authors have read and agreed to the published version of the manuscript.

FUNDING

This work was supported by the Natural Science Foundation of Chongqing City of China (Grant Nos. cstc2019jcyj-zdxmX0024, cstc2019jcyj-msxmX0507, and cstc2020jcyj-msxmX0216), the Technological Research Program of Chongqing Municipal Education Commission (Grant No. KJQN20200), and in part by the Bayu Scholars Program.

SUPPLEMENTARY MATERIAL

The Supplementary Material for this article can be found online at: https://www.frontiersin.org/articles/10.3389/fenrg.2021.813978/full#supplementary-material

REFERENCES

Abass, H., Sierra, L., and Tahini, A. (2009). "Optimizing Proppant Conductivity and Number of Hydraulic Fractures in Tight Gas Sand wells," in SPE Saudi Arabia Section Technical Symposium, 126159. doi:10.2118/126159-MS

Ao, X., Qi, Z., Xiang, Z., Li, Z., Qu, H., and Wang, Z. (2020). Swelling of Shales by Supercritical Carbon Dioxide and its Relationship to Sorption. *ACS Omega* 5 (31), 19606–19614. doi:10.1021/acsomega.0c02118

Ao, X., Wang, B., Qu, H., Xiang, Z., and Luo, Z. (2021). Swelling of Shales with Slickwater in Carbon Dioxide. *Energy Fuels* 35 (6), 5122–5129. doi:10.1021/acs.energyfuels.0c04315

Boyer, J., Maley, D., and O'Neil, B. (2014). "Chemically Enhanced Proppant Transport," in SPE Annual Technical Conference and Exhibition, 170640. doi:10.2118/170640-MS

Chen, H., Zhou, T., Fan, H. C., Zhang, J., and Yang, S. L. (2020). Preparation Method and Stress Sensitivity of Artificial Fracture Rock Sample in Shale Reservoir. *J. Pet.* 41 (09), 1117–1126.

Chen, M., Zhang, S. C., Liu, M., Ma, X. F., and Zou, Y. S. (2018). Calculation Method of Proppant Embedment Depth in Hydraulic Fracturing. *Pet. Exploration Dev.* 45 (01), 149–156. doi:10.1016/s1876-3804(18)30016-8

Deng, S. C., Zuo, H., Li, H. B., Huang, Z. H., Xiao, C. X., Zeng, Y. Q., et al. (2017). Numerical Investigation of Flow Conductivity of Propping Agent in Hydraulic Fracture under *In-Situ* Stresses. *J. Coal* 42 (S2), 434–440. doi:10.13225/j.cnki.jccs.2017.0687

Guo, J. C., Lu, C., Zhao, J. Z., and Wang, W. Y. (2008). Experimental Research on Proppant Embedment. *J. Coal* (06), 661–664.

Guo, T. K., and Zhang, S. C. (2011). Study on the Factors Affecting Proppant Embedment. *Fault Block Oil and Gas Field* 18 (04), 527–529+544.

He, S. Y., Zhao, L. Q., Luo, Z. F., Li, J., and Li, H. (2018). Study on Indoor Gas Measurement of Supporting Fracture Conductivity of Tight sandstone. *Oil Gas Reservoir Eval. Dev.* 8 (06), 45–50. doi:10.13809/j.cnki.cn32-1825/te.2018.06.009

Lei, Q., Weng, D. W., Guan, B. S., Mu, L. J., Xu, Y., Wang, Z., et al. (2020). A Novel Approach of Tight Oil Reservoirs Stimulation Based on Fracture Controlling Optimization and Design. *Pet. Exploration Dev.* 47 (03), 592–599. doi:10.1016/s1876-3804(20)60080-5

Lei, Y., Zeng, Y., and Ning, Z. f. (2018). Transient Flow Model of Multiply Fractured Horizontal wells in Shale Gas Reservoirs and Well Test Analysis. *Fault Block Oil and Gas Field* 25 (04), 477–483.

Li, N., Li, J., Zhao, L., Luo, Z., Liu, P., and Guo, Y. (2016). "Laboratory Testing and Numeric Simulation on Laws of Proppant Transport in Complex Fracture Systems," in SPE Asia Pacific Hydraulic Fracturing Conference, 181822. doi:10.2118/181822-MS

Liu, W., Zhao, H., Lei, Z. X., Chen, Z. S., Cao, L., Zhang, K., et al. (2019). Reservoir Assisted History Matching Method Using a Local Ensemble Kalman Filter Based on Single-Well Sensitivity Region. *J. Pet.* 40 (06), 716–725.

Liu, X. W. (2020). Influencing Factors of Hydraulic Propped Fracture Conductivity in Shale Reservoir. *Fault Block Oil and Gas Field* 27 (03), 394–398.

Rivers, M., Zhu, D., and Hill, A. D. D. (2012). "Proppant Fracture Conductivity with High Proppant Loading and High Closure Stress," in SPE Hydraulic Fracturing Technology Conference, 151972. doi:10.2118/151972-MS

Sun, Y. W., Hao, Y. C., Wang, Y. L., Dong, S. X., and Peng, G. W. (2019). Study on Optimum Design Method of Hydraulic Fracture Parameters in Shale Gas Reservoir. *J. Sheng Li CollegeChina Univ. Pet.* 33 (02), 24–27.

Tan, Y., Pan, Z., Liu, J., Wu, Y., Haque, A., and Connell, L. D. (2017). Experimental Study of Permeability and its Anisotropy for Shale Fracture Supported with Proppant. *J. Nat. Gas Sci. Eng.* 44, 250–264. doi:10.1016/j.jngse.2017.04.020

Wang, Y. D., Ren, Y., Zheng, B., Gong, R. R., Niu, S. L., Chen, L., et al. (2020). Study on the Influencing Factors of Proppant Embedment in Hydraulic Fracturing of Shale Reservoir. *Drilling Prod. Tech.* 43 (04), 129–132.

Wen, Q. Z., Zhang, S. C., Wang, L., and Liu, Y. S. (2005). Influence of Proppant Embedment on Fracture Long-Term Flow Conductivity. *Nat. Gas Industry* 25 (5), 65–68.

Xu, G. Q., Zhang, S. C., Wang, Lei., and Han, J. Y. (2011). Influence Factors Analysis of Proppant Fracture in Channel Fracturing. *Fault Block Oil and Gas Field* 18 (04), 527–529+544.

Xu, J., Ding, Y., Yang, L., Liu, Z., Gao, R., Yang, H., Yang, H. X., et al. (2019). Effect of Proppant Deformation and Embedment on Fracture Conductivity after Fracturing Fluid Loss. *J. Nat. Gas Sci. Eng.* 71, 102986. doi:10.1016/j.jngse.2019.102986

Yang, Z.-z., Liao, Z.-j., Li, X.-g., Yi, L.-p., Chen, H., and Ran, L. (2021). A Model to Calculate Fracture Conductivity Considering Proppant Transport and Embedment Depth. *Chem. Technol. Fuels Oils* 57 (3), 499–517. doi:10.1007/s10553-021-01273-4

Zeng, B., Wang, X. H., Huang, H. Y., Zhang, N. Q., Yue, W. H., Deng, Q., et al. (2020). Key Technology of Volumetric Fracturing in Deep Shale Gas Horizontal wells in Southern Sichuan. *Pet. Drilling Tech.* 48 (05), 77–84.

Zeng, L. X. (2020). Analysis of Key Stimulation Parameters for Shale Gas Horizontal wells. *Well Test.* 29 (05), 27–32. doi:10.19680/j.cnki.1004-4388.2020.05.005

Zhao, Y. D., Zhang, S. A., Xiao, F. C., He, J. Y., Dong, Y. T., Zhao, W., et al. (2017). Experimental Study on Long-Term Flow Conductivity of Fractured Fractures in Different Types of Reservoirs. *Sci. Tech. Eng.* 17 (11), 192–197.

Conflict of Interest: The authors declare that the research was conducted in the absence of any commercial or financial relationships that could be construed as a potential conflict of interest.

Publisher's Note: All claims expressed in this article are solely those of the authors and do not necessarily represent those of their affiliated organizations, or those of the publisher, the editors, and the reviewers. Any product that may be evaluated in this article, or claim that may be made by its manufacturer, is not guaranteed or endorsed by the publisher.

Copyright © 2022 Xiang, Ding, Ao, Zhong, Li, Xiao, Chen, Xiao and Ma. This is an open-access article distributed under the terms of the Creative Commons Attribution License (CC BY). The use, distribution or reproduction in other forums is permitted, provided the original author(s) and the copyright owner(s) are credited and that the original publication in this journal is cited, in accordance with accepted academic practice. No use, distribution or reproduction is permitted which does not comply with these terms.